

Domain Walls in Non-Equilibrium Systems and the Emergence of Persistent Patterns

Aric Hagberg and Ehud Meron

Arizona Center for Mathematical Sciences
and Program in Applied Mathematics
University of Arizona
Tucson, AZ 85721

Abstract:

Domain walls in equilibrium phase transitions propagate in a preferred direction so as to minimize the free energy of the system. As a result, initial spatio-temporal patterns ultimately decay toward uniform states. The absence of a variational principle far from equilibrium allows the coexistence of domain walls propagating in any direction. As a consequence, *persistent* patterns may emerge. We study this mechanism of pattern formation using a non-variational extension of Landau's model for second order phase transitions.

PACS numbers: 05.70.Fh, 42.65.Pc, 47.20.Ky, 82.20Mj

Second order phase transitions, such as in ferromagnets or liquid-vapor systems, are manifestations of spontaneous symmetry breaking occurring near thermal equilibrium. The coexistence of broken symmetry states beyond the transition point gives rise to spatial patterns consisting of domain walls or fronts separating regions of different phase. The dynamics of domain walls near thermal equilibrium, are dictated by a variational principle, namely, the minimization of the free energy. As a consequence, initial spatio-temporal patterns ultimately decay toward the stationary homogeneous states of lowest free energy. Front structures are commonly observed in far-from-equilibrium systems as well. Walls separating conductive and convective states in binary mixtures [1], excited and recovery regions in autocatalytic chemical reactions [2], or different phase-locked states in parametrically forced surface waves [3], are a few examples. Unlike equilibrium systems, however, no general variation principle, like the minimization of free energy, applies for systems maintained far from equilibrium. The possible outcome, as emphasized recently [4-7], is the appearance of localized structures and, more generally, persistent spatio-temporal patterns.

In this paper we further elaborate on pattern formation as a non-variational effect. We consider spatio-temporal patterns involving domain walls and show that multiplicity of stable front solutions may give rise to persistent patterns. As a model system we choose to study a non-variational extension of the Landau-Ginzburg model for a scalar order parameter. The extended system takes the form of coupled reaction diffusion equations that have extensively been studied in the context of chemical and biological patterns [8-13]. Some of the results to be described here have already been obtained in that context before, particularly by Rinzel and Terman [12]. We rederive these results and present them here in a way that best illustrates the different point of view we put forward in this paper.

Consider a variational system whose free energy (Liapunov functional) is given by

$$\mathcal{F} = \int [\mathcal{U}(\phi, h) + \phi_x^2/2] dx, \quad (1)$$

where $\mathcal{U}(\phi, h) = -\phi^2/2 + \phi^4/4 + h\phi$, $\phi(x, t)$ is a scalar order parameter, h is a constant

bias field and the subscript x denotes the spatial partial derivative. For h values in the range $-2/(3\sqrt{3}) < h < 2/(3\sqrt{3})$ the free energy density, \mathcal{U} , has a double-well form. The two wells correspond to stationary homogeneous states, characterized by order-parameter values $\phi_-(h)$ and $\phi_+(h)$ that solve the cubic equation $\phi^3 - \phi + h = 0$. The relaxation toward any of these stationary states is governed by the equation $\phi_t = -\delta\mathcal{F}/\delta\phi$, or

$$\phi_t = f(\phi, h) + \phi_{xx} \quad f(\phi, h) = \phi - \phi^3 - h. \quad (2)$$

Front solutions, $\phi = \phi(\chi)$ where $\chi = x - ct$, of (2) [14] propagate in a preferred direction dictated by the minimization of \mathcal{F} . The speed of a front connecting $\phi_+(h)$ at $\chi = -\infty$ to $\phi_-(h)$ at $\chi = \infty$ is given by

$$c = \mu(h) = \alpha[\mathcal{U}(\phi_-) - \mathcal{U}(\phi_+)], \quad (3)$$

where $\alpha(h) = 1/\int_{-\infty}^{\infty} \phi'(h)^2 d\chi$ is positive [11]. For negative h values, $\mathcal{U}(\phi_-) > \mathcal{U}(\phi_+)$ and the front moves in the positive x direction ($c > 0$) so as to increase that part of the system having lower energy. When h is positive the front propagates toward negative x values ($c < 0$). Notice that (2) remains invariant under the transformation $x \rightarrow -x$. Thus, in addition to a front connecting $\phi_+(h)$ to $\phi_-(h)$ and propagating, say, at positive speed c , there exists a symmetric front connecting $\phi_-(h)$ to $\phi_+(h)$ and propagating at a negative speed $-c$. In the following we refer to these symmetric solutions as representing the same type of front solution.

Imagine now that h is not constant but, instead, a second field $h = h(x, t)$ coupled to $\phi = \phi(x, t)$. A variety of physical, chemical and biological systems fall in that category. Bistable optical systems [15], crystal growth [16], autocatalytic chemical reactions [2,8], and predator-prey systems [17], are a few examples. For the present purposes it is sufficient to consider the simplest case where $h(x, t)$ is a diffusive field that responds linearly to changes in the order parameter $\phi(x, t)$. More specifically we assume the form [8]

$$h_t = \epsilon g(\phi, h) + \delta h_{xx} \quad g(\phi, h) = \phi - a_0 - a_1 h, \quad (4)$$

where $\epsilon > 0$ is the ratio, τ_ϕ/τ_h , between the time scales associated with the two fields ϕ and h , $\delta = D_h/D_\phi$ is the ratio of diffusion constants, and the coefficient a_1 is positive. The combined system (2) and (4) (denoted hereafter by (2+4)) is no longer variational. Yet, it resembles the original system (2) in having, for a proper choice of a_0 and a_1 , three stationary homogeneous solutions of which two are stable. The stable solutions correspond to the intersection points of the nullcline $g(\phi, h) = 0$ with the branches $\phi = \phi_\pm(h)$ and are denoted here by (ϕ_\pm, h_\pm) (see Figs. 1). Unlike the variational system, however, the two stable states can be connected by more than one type of front solutions when ϵ is sufficiently small [10-13]. Preparing the system at the lower state (ϕ_-, h_-) and perturbing it locally so as to induce a transition to the upper branch $\phi = \phi_+(h)$, yields a front propagating to the right: $(\phi(\chi), h(\chi)) \rightarrow (\phi_\pm, h_\pm)$ as $\chi \rightarrow \mp\infty$, $c > 0$. If, on the other hand, the initial state is the upper one, (ϕ_+, h_+) , a perturbation that induces a transition to the lower branch $\phi = \phi_-(h)$ yields a front connecting the same asymptotic states but propagating to the left: $(\phi(\chi), h(\chi)) \rightarrow (\phi_\pm, h_\pm)$ as $\chi \rightarrow \mp\infty$, $c < 0$. The two fronts are not related by the symmetry $x \rightarrow -x$ and, therefore, represent two different types of front solutions.

The multiplicity of front solutions and the symmetry $x \rightarrow -x$ of (2) imply that along with a front that transforms the lower state (ϕ_-, h_-) to the upper state (ϕ_+, h_+) , there exists another front (hereafter “back”) propagating in the *same direction* that transforms the upper state back to the lower one. A combination of the two may yield a persistent localized structure, provided there exists a mechanism which binds the back to the front.

To study the emergence of such a structure we consider the small ϵ regime, $\epsilon \ll 1$, and assume a nondiffusive h field, or $\delta = 0$ (allowing diffusion of h will not affect the results qualitatively as long as δ is not too large). We then distinguish between front and back regions where h barely changes, and outer regions where ϕ can be eliminated adiabatically, $\phi = \phi_\pm(h)$ [8-10]. Imagine now a front transforming the down state (ϕ_-, h_-) into the upper one (ϕ_+, h_+) and propagating to the right. The front speed is determined by the

local value of h : $c = \mu(h_-) > 0$. A back that follows the front (so as to form a single up-state domain) will be affected by the field $h(\chi)$ that develops behind the front. This field, as we will show below, provides the binding force the front exerts on the back. In order to find that field we insert $\phi = \phi_+(h)$ in (4) to obtain a closed equation for h , and use the boundary conditions $h(\chi_f^0) = h_-$ and $h(\chi) \rightarrow h_+$ as $\chi \rightarrow -\infty$, where χ_f^0 denotes the front position in a frame moving at speed c . Solving for h we find

$$h(\chi) = (h_- - h_+)e^{\epsilon\kappa(\chi - \chi_f^0)} + h_+ \quad \chi \leq \chi_f^0, \quad (5)$$

where $h_{\pm} = 2(\pm 1 - a_0)/(1 + 2a_1)$ and $\kappa = (a_1 + 1/2)/c$. In deriving (5) we used the linear approximation $\phi_{\pm}(h) \approx \pm 1 - h/2$ valid for small $|h|$.

For an up-state domain to become a localized structure of fixed size, the back speed should be equal to the front speed c . We thus require $\mu(h_b^0) = -c$, where $h_b^0 = h(\chi_b^0)$ is the local value of h at the back. This relation determines h_b^0 . Note that h_b^0 must be positive, whereas h_- , the value of h at the front, is negative. Inserting $h = h_b^0$ and $\chi = \chi_b^0$ in (5) we find for the size of the localized structure

$$\lambda = \chi_f^0 - \chi_b^0 = \frac{1}{\epsilon\kappa} \ln\left(\frac{h_+ - h_-}{h_+ - h_b^0}\right). \quad (6)$$

According to (6), a localized structure of fixed size exists for $h_+ > h_b^0$ (for $h_+ < h_b^0$ the front speed is larger than the back speed and the up-state domain expands indefinitely). We will now show that this structure is also stable to translational perturbations. To this end we represent the back in the form

$$\phi_b(x, t) = \phi_b^0(\chi - \chi_b) + \epsilon\phi_b^1(\chi - \chi_b, \epsilon t),$$

where $\chi_b = \chi_b^0 + \tilde{\chi}_b(\epsilon t)$ is the actual back position, and write the level of h at the back as $h_b = h(\chi_b) = h_b^0 + \epsilon h_b^1(\epsilon t)$. Using these forms in (2), assuming h is constant across the back, we find

$$\partial_{\chi}^2 \phi_b^1 + c\partial_{\chi} \phi_b^1 + (1 - 3\phi_b^0)^2 \phi_b^1 = h_b^1 - \epsilon^{-1} \dot{\chi}_b \frac{d\phi_b^0}{d\chi}, \quad (7)$$

where the dot over χ_b denotes differentiation with respect to t . Solvability of (7) requires the right hand side of that equation to be orthogonal to $(d\phi_b^0/d\chi)\exp(c\chi)$. This leads to

$$\dot{\chi}_b = \beta\epsilon h_b^1, \quad (8)$$

where β is a positive constant. Using (5) to evaluate $h_b = h(\chi_b)$ and consequently ϵh_b^1 we find from (8)

$$\dot{\tilde{\chi}}_b = \beta(h_+ - h_b^0)(1 - e^{\epsilon\kappa\tilde{\chi}_b}). \quad (9)$$

The linearization of (9) about $\tilde{\chi}_b = 0$ gives the equation $\dot{\tilde{\chi}}_b = -\epsilon\kappa\beta(h_+ - h_b^0)\tilde{\chi}_b$. Since $\kappa > 0$, we conclude that for $\epsilon \ll 1$, a stable localized structure is formed whenever $h_+ > h_b^0$.

We consider now the other extreme, $\epsilon \gg 1$. Adiabatic elimination of h reduces (2+4) to the variational equation

$$\phi_t = (1 - a_1^{-1})\phi - \phi^3 + a_0/a_1 + \phi_{xx} \quad (10)$$

with $h = \phi/a_1 - a_0/a_1$, where we assumed that $\delta \ll \epsilon$. Equation (10) is equivalent to (2) and, consequently, has only one type of front solution connecting the two states (ϕ_{\pm}, h_{\pm}) . When $a_0 = 0$ the system (2+4) has an odd symmetry about $(\phi, h) = (0, 0)$. The two states (ϕ_{\pm}, h_{\pm}) are equally stable and the front that connects them is stationary. When $\delta = 0$ it becomes an exact solution of (2+4) that exists for all ϵ values. Fig. 1a shows a phase portrait of this front solution in the (ϕ, h) plane. It amounts to a straight diagonal line, $h = a_1^{-1}\phi$, connecting the two states. We recall that for $\epsilon \ll 1$ equations (2+4) admit two types of propagating solutions. One may therefore expect to find a bifurcation from a single to multiple front solutions as ϵ is decreased [12].

To study this bifurcation we consider the symmetric model ($a_0 = 0$) with a non-diffusive h field and write a propagating front solution, $\phi = \phi_p(x - ct)$, $h = h_p(x - ct)$, as power series in c

$$\begin{aligned} \phi_p &= \phi_s + c\phi_1 + c^2\phi_2 + \dots \\ h_p &= h_s + ch_1 + c^2h_2 + \dots, \end{aligned} \quad (11)$$

where $(\phi_s, h_s = a_1^{-1}\phi_s)$ is the stationary front solution. Expanding ϵ as well, $\epsilon = \epsilon_0 + c\epsilon_1 + c^2\epsilon_2 + \dots$, and using these expansions in (2+4) (with $a_0 = \delta = 0$) we find solvability conditions, one at each order, that determine the coefficients $\epsilon_0, \epsilon_1, \dots$. Carrying out this perturbation scheme to third order in c we find $\epsilon_0 = a_1^{-2}$, $\epsilon_1 = 0$ and $\epsilon_2 < 0$. These results imply a supercritical pitchfork bifurcation occurring at $\epsilon_c = \epsilon_0 = a_1^{-2}$. Near the bifurcation the front speed scales like $c \sim (\epsilon_c - \epsilon)^{1/2}$. Numerical studies on (2+4) confirm these results. A numerically computed bifurcation diagram for the symmetric case $a_0 = 0$ is shown in Fig. 2a.

The leading order corrections in (11) take the form $\phi_1 = 0$, $h_1 = \phi'_s$. Using these forms in (11) we see that the difference between the stationary and the counter propagating solutions close to the bifurcation point is that in the latter the field h is *translated* to the right or to the left by an amount proportional to c . This translation breaks the odd symmetry of the stationary solution and gives rise to phase portraits deviating from the diagonal, $h = a_1^{-1}\phi$, as shown in Fig. 1b. The speed c can be directly related to this deviation by using (11):

$$c = \alpha_s \int_{-\infty}^{\infty} \psi \phi'_s d\chi \quad \psi = h_p - a_1^{-1}\phi_p, \quad (12)$$

where $\alpha_s = 1/\int_{-\infty}^{\infty} (\phi'_s)^2 d\chi$ is positive. Thus a front connecting (ϕ_+, h_+) at $\chi = -\infty$ to (ϕ_-, h_-) at $\chi = \infty$ propagates to the right ($c > 0$) when the deviation from the diagonal is negative ($\psi < 0$) and to the left when the deviation is positive ($\psi > 0$). As before, we refer to the latter case as describing a back.

A significant distinction between the stationary front solution $\phi = \phi_s$, $h = a_1^{-1}\phi_s$ (in the symmetric model) and the two propagating solutions $\phi = \phi_s$, $h = a_1^{-1}\phi_s \pm c\phi'_s$ that bifurcate at $\epsilon = \epsilon_c$ can be made by looking at the phase $\theta = \arctan(h/\phi)$. Across the stationary front the phase remains constant everywhere except for the core where it suffers a jump of π as the fields ϕ and h vanish and change sign. Across a propagating front, on the other hand, the phase smoothly rotates by π keeping the modulus $(\phi^2 + h^2)^{1/2}$ nonzero.

Similar types of walls have been found in the context of anisotropic ferromagnets [18] and, recently, in a nonvariational model describing a periodically forced oscillating medium [19] (see also Refs. [20,21]). They are referred to as Ising walls when the phase is singular and as Bloch walls when the phase rotates smoothly.

The symmetric model is nongeneric unless the relevant physics dictates an odd symmetry. Unfolding the symmetric case by allowing non zero values of a_0 yields a bifurcation diagram as shown in Fig. 2*b*. In that case, front multiplicity arises by a saddle node bifurcation occurring at $\epsilon_{sn}(a_0) < \epsilon_c$. For small a_0 we find the scaling behavior, $\epsilon_c - \epsilon_{sn} \sim |a_0|^{1/2}$.

In the small ϵ regime we could show, using leading order singular perturbation analysis, that front multiplicity gives rise to persistent patterns. We postpone the analogous analysis for higher ϵ values to a subsequent study and present here, instead, results of direct numerical integration of (2+4) (with $\delta = 0$). Our observations are summarized in a phase diagram shown in Fig. 3 (see also Fig. 6 of Ref. [12]). To the right of the solid curve $\epsilon = \epsilon_{sn}(a_0)$ only one type of front solution exists and, as we expect, initial patterns decay toward a uniform state. We note that along the line $a_0 = 0$ the decay can be extremely slow and unnoticeable in practical situations [22]. As we cross the solid curve by decreasing ϵ below $\epsilon_{sn}(a_0)$ front multiplicity arises. For some range of ϵ initial patterns still decay toward a uniform state. Persistent patterns, in the form of stable solitary and periodic traveling waves, appear below a second critical value of ϵ , that is, in the region to the left of the dashed curve.

We have presented here a mechanism of pattern formation in systems undergoing a bifurcation from Ising to Bloch type fronts. A key ingredient in this mechanism is the coexistence of stable, counter propagating front solutions connecting the same asymptotic states as $|\chi| \rightarrow \infty$. Coexistence of such fronts cannot occur in variational systems having free energies. The mechanism can be tested in bistable chemical reactions [2].

We would like to thank Rob Indik and Joceline Lega for interesting discussions. We also wish to thank the Arizona Center for Mathematical Sciences (ACMS) for support.

ACMS is sponsored by AFOSR contract FQ8671-9000589 (AFOSR-90-0021) with the University Research Initiative Program at the University of Arizona. Part of this work has been done while A.H. was visiting the Center for Nonlinear Studies at Los Alamos National Laboratory and E.M. the Chemical Physics Department at the Weizmann Institute. We thank these places for their warm hospitalities.

References:

1. E. Moses, J. Feinberg and V. Steinberg, Phys. Rev. A **35**, 2757 (1987); R. Heinrichs, G. Ahlers and D. S. Cannell, Phys. rev. A **35**, 2761 (1987); P. Kolodner, D. Bensimon and C. M. Surko, Phys. Rev. Lett. **60**, 1723 (1988); K. E. Anderson and R. P. Behringer, Phys. Lett. **145**, 323 (1990); H. Riecke, Phys. Rev. Lett. **68**, 301 (1992).
2. R. J. Field and M. Burger, *Oscillations and Traveling Waves in Chemical Systems* (Wiley, New York, 1985). See also Refs. [8] below.
3. C. Elphick and E. Meron, Phys. Rev. A **40**, 3226 (1989); B. Denardo, W. Wright and S. Putterman, Phys. Rev. Lett. **64**, 1518 (1990).
4. O. Thual and S. Fauve, J. Phys. (Paris) **49**, 1829 (1988); S. Fauve and O. Thual, Phys. Rev. Lett. **64**, 282 (1990).
5. V. Hakim, P. Jakobsen and Y. Pomeau, Europhys. Lett. **11**, 19 (1990); Y. Pomeau, Physica D **51**, 546 (1991).
6. W. van Saarloos and P. C. Hohenberg, Phys. Rev. Lett. **64**, 749 (1990); Physica D **56**, 303 (1992).
7. T. Ohta and M. Mimura, in *Formation, Dynamics and Statistics of Patterns I*, eds. K. Kawasaki, M. Suzuki and A. Onuki (World Scientific, New York, 1990).
8. J. J. Tyson and J. P. Keener, Physica D **32**, 327 (1988); A. S. Mikhailov, *Foundation of Synergetics I. Distributed Active Systems* (Springer, Berlin, 1990); E. Meron, “Pattern Formation in Excitable Media”, to appear in Physics Reports.
9. P. C. Fife, CBMS-NSF Regional Conf. Series in Appl. Math. **53**, 1 (1988).
10. P. Ortoleva and J. Ross, J. Chem. Phys. **63**, 3398 (1975).
11. P. C. Fife, J. Chem. Phys. **64**, 554 (1976).
12. J. Rinzel and D. Terman, SIAM J. Appl. Math. **42** 1111 (1982).
13. H. Ikeda, M. Mimura and Y. Nishiura, Nonl. Anal. TMA **13**, 507 (1989).
14. D. G. Aronson and H. F. Weinberger in *Proceedings of the Tulane Program in Partial Differential Equations and Related Topics*, ed. J. Goldstein (Springer, Berlin, 1975).

15. J. L. Jewell, H. M. Gibbs, S. S. Tarnag, A. C. Gossard, and W. Weigmann, *Appl. Phys. Lett.* **40**, 291 (1982); E. Abraham, *Optics Communications* **61**, 282 (1987).
16. J. B. Collins and H. Levine, *Phys. Rev.* **B31**, 6119 (1985); G. Caginalp, *Ann. Phys.* **172**, 136 (1986).
17. J. D. Murray, *Mathematical Biology* (Springer, New York, 1989).
18. J. Lajzerowicz and J. J. Niez, *J. Phys (Paris) Lett.* **40** L165 (1979).
19. P. Couillet, J. Lega, B. Houchmanzadeh, and J. Lajzerowicz, *Phys. Rev. Lett.* **65** 1352 (1990).
20. S. Sarker, S. E. Trullinger, and A. R. Bishop, *Phys. Lett.* **59A**, 255 (1976).
21. P. Couillet, J. Lega, and Y. Pomeau, *Europhys. Lett.* **15**, 221 (1991).
22. K. Kawasaki and T. Ohta, *Physica* **116A**, 573 (1982); J. Carr and R. L. Pego, *Comm. Pure and Appl. Math.* **42**, 523 (1989).

Figure Captions:

Figure 1: Phase portraits of front solutions connecting the (ϕ_+, h_+) state at $\chi = -\infty$ to the (ϕ_-, h_-) state at $\chi = \infty$. The light colored curves are the nullclines $f = 0$ and $g = 0$ and the dark colored curves are the numerically computed trajectories. The computational parameters are: a. $\epsilon = 1.0$, $\delta = 0$, $a_1 = 2.0$, $a_0 = 0$. b. $\epsilon = .2$, $\delta = 0$, $a_1 = 2.0$, $a_0 = 0$. c.

Figure 2: Bifurcation diagrams of front solutions. The dots are data points representing the speed of the different types of stable front solutions that exist for each value of ϵ . a. The symmetric case ($a_0 = 0$). b. The nonsymmetric case ($a_0 = .1$).

Figure 3: Phase diagram in the $\epsilon - a_0$ plane. For the region to the right of the solid curve only one type of front solution exists and initial patterns do not persist. In the region between the solid and the dashed curves multiple stable fronts coexist but patterns still decay toward a uniform state. For the region to the left of the dashed curve initial patterns evolve toward persistent patterns in the form of stable traveling waves. Computational parameters are : $\delta = 0$, $a_1 = 2.0$.

Figure 1a

h

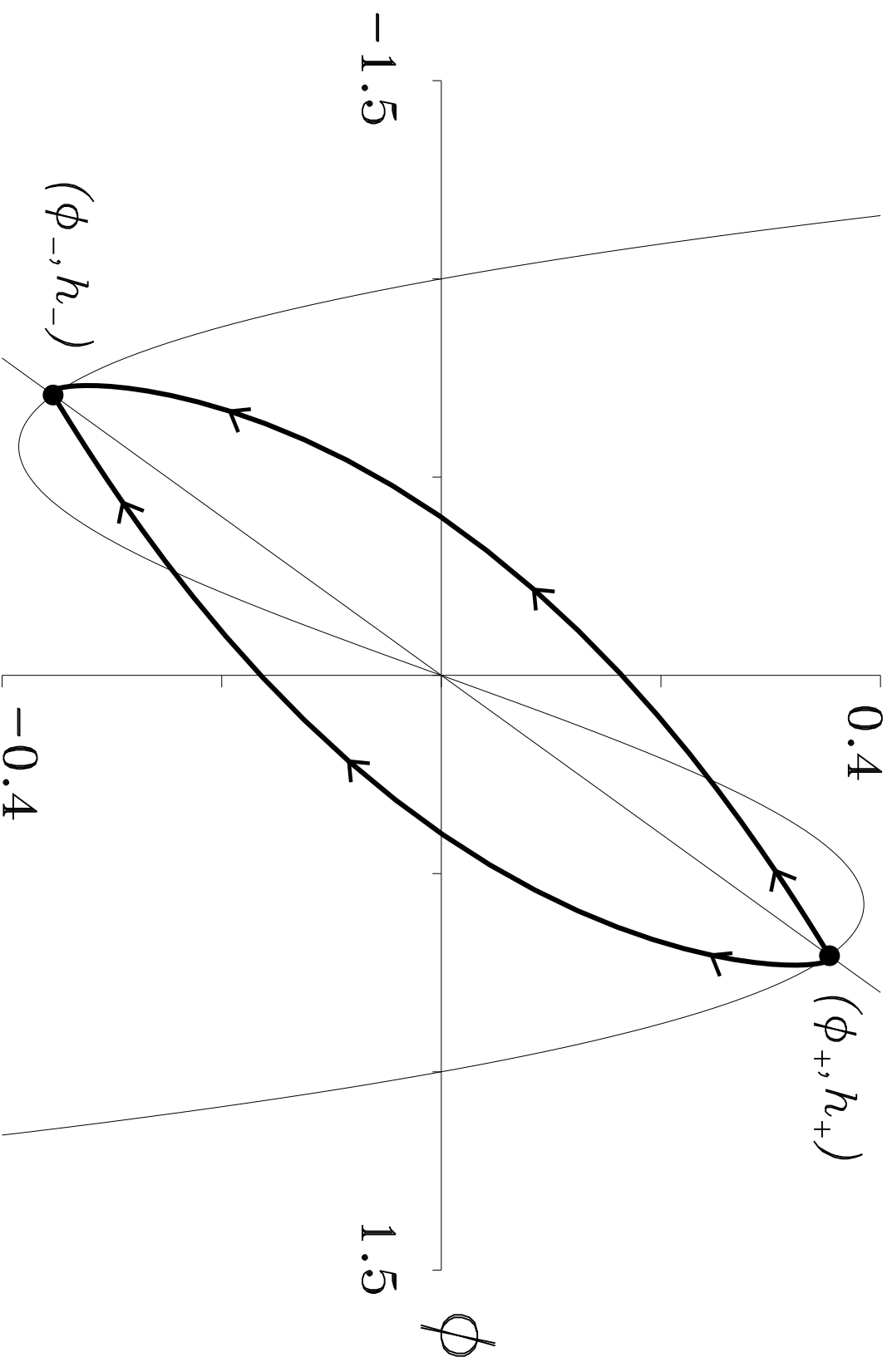


Figure 1b

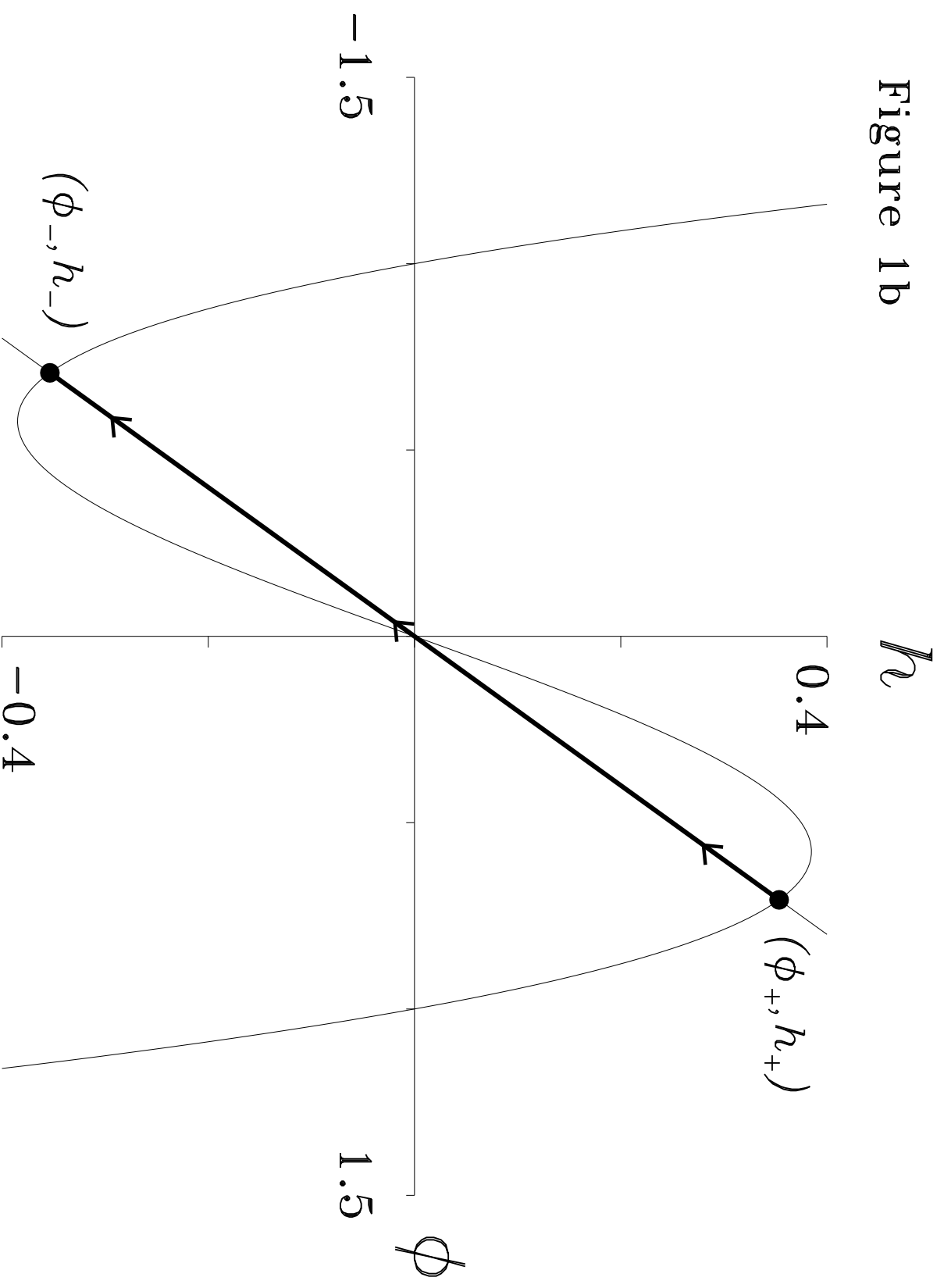


Figure 2a

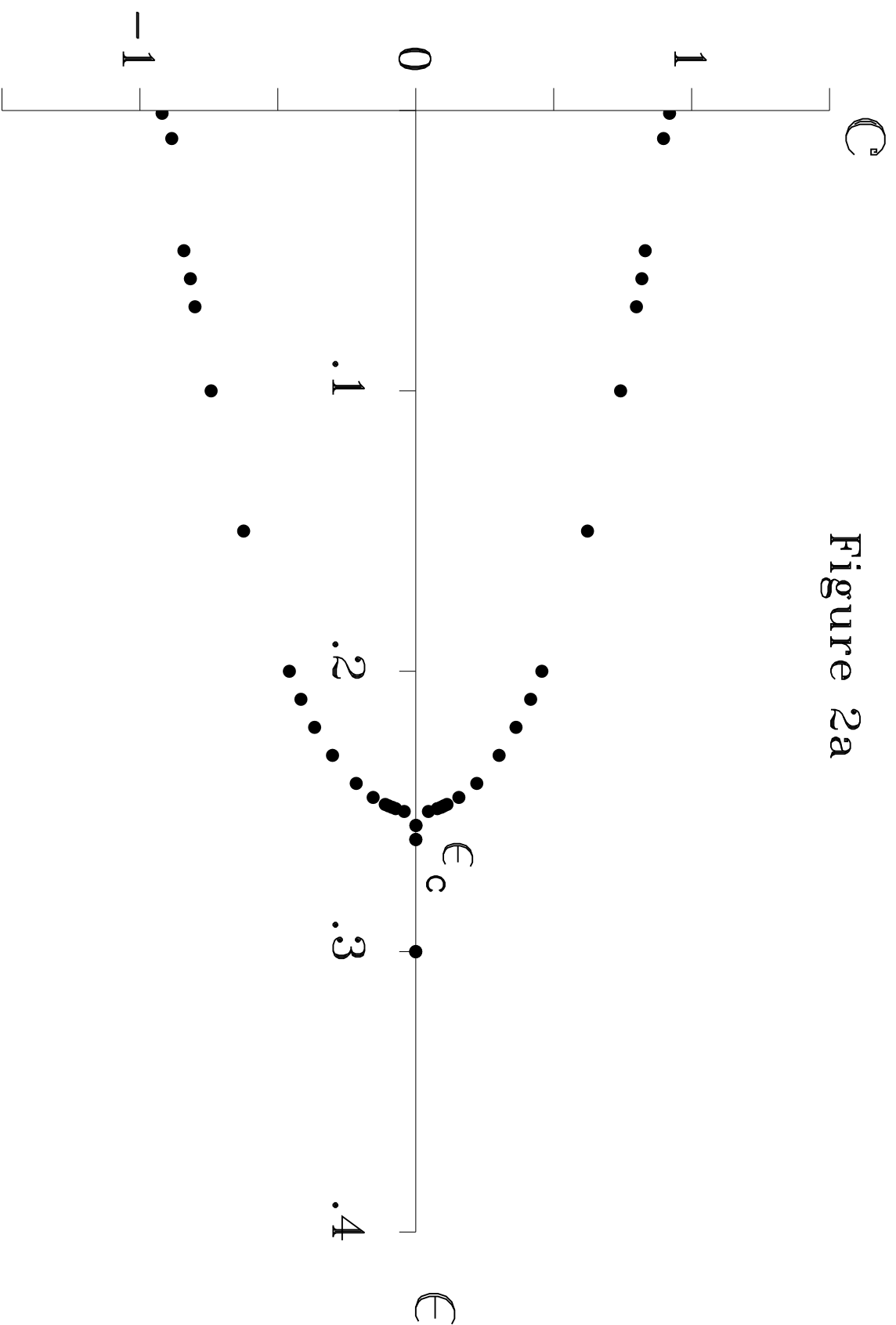


Figure 2b

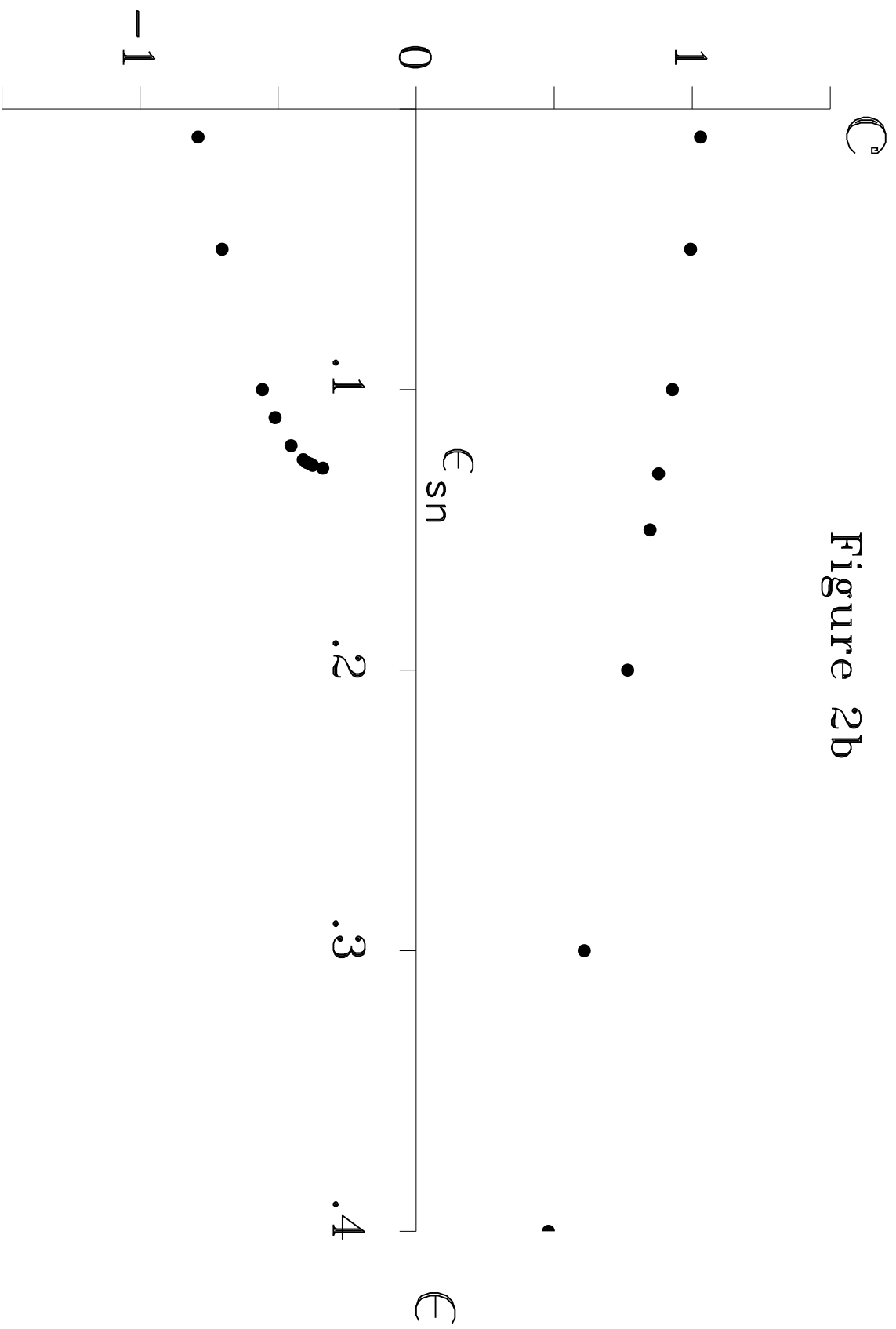


Figure 3

